



REVIEW

Electrophoretically deposited hydroxyapatite-based composite coatings loaded with silver and gentamicin as antibacterial agents

MILENA STEVANOVIĆ^{1#}, MARIJA DJOŠIĆ^{2#}, ANA JANKOVIĆ^{1#},
KYONG YOP RHEE³ and VESNA MIŠKOVIĆ-STANKOVIĆ^{1**#}

¹Faculty of Technology and Metallurgy, University of Belgrade, Karnegijeva 4, 11000 Belgrade, Serbia, ²Institute for Technology of Nuclear and Other Mineral Raw Materials (ITNMS), Bulevar Franš d'Epereia 86, Belgrade, Serbia and ³Department of Mechanical Engineering, Kyung Hee University, Yongin 449-701, South Korea

(Received 21 August, accepted 28 August 2019)

Abstract: Increasing need for improved, compatible bone tissue implants led to the intensive research of novel biomaterials, especially hydroxyapatite (HAP)-based composite materials on titanium and titanium alloy surfaces. Owing to its excellent biocompatibility and osteoinductivity properties, hydroxyapatite is often used as part of composite biomaterials aimed for orthopedic implant applications. In order to overcome persistent problems of bacterial infection, various antimicrobial agents and materials and their incorporation in such medical devices were investigated. This paper represents a comprehensive review of single-step electrodeposition on titanium of hydroxyapatite/chitosan/graphene composite coatings loaded with silver and antibiotic gentamicin as antibacterial agents. The improvement of mechanical and adhesive properties of deposited composite coatings was achieved by graphene and chitosan addition, while desirable antibacterial properties were introduced by including antibiotic gentamicin and silver. The biocompatibility of electrodeposited HAP and HAP-based composite coatings was evaluated by MTT testing, indicating a non-cytotoxic effect and high potential for future medical use as orthopedic implant coating.

Keywords: electrophoretic deposition; composite; hydroxyapatite; bone implants; antibacterial coating.

* Corresponding author. E-mail: vesna@tmf.bg.ac.rs
Serbian Chemical Society member.
<https://doi.org/10.2298/JSC190821092S>

CONTENT

1. INTRODUCTION
2. ELECTROPHORETIC DEPOSITION OF HYDROXYAPATITE-BASED COMPOSITE COATINGS ON TITANIUM
 - 2.1. FTIR analysis
 - 2.2. FE-SEM analysis
 - 2.3. XPS analysis
 - 2.4. TG analysis
 - 2.5. Antibacterial activity
 - 2.6. Cytotoxicity
3. CONCLUSION

1. INTRODUCTION

Electrophoretic deposition (EPD) is a versatile technique that allows obtaining of multifunctional thin films and coatings.¹ The main advantages are simplicity and efficiency of the process since it allows for room temperature manufacturing, as well as the thickness, porosity and composition control of deposited films.² Coatings obtained by EPD technique are characterized as homogenous, porous and often with good adhesion properties and therefore suitable for various purposes, including the coatings for biomedical applications.^{3–7} EPD of hydroxyapatite (HAP)-based composite coatings has gained much attention in the biomedical field.⁸ HAP is a ceramic biomaterial with a chemical composition similar to natural bone and characterized by outstanding biocompatibility and osteoinductivity which is especially interesting from the standpoint of developing orthopedic implants.⁹ The ability to promote osseointegration process and to establish a direct chemical bond of the implant to the bone tissue, makes HAP as a perfect candidate for designing implant devices.¹⁰ On the other side, the HAP brittleness and pure mechanical properties have imposed a need for the development of HAP coatings on an appropriate substrate that could provide mechanical support.¹¹ Commercially pure Ti and its alloys (*e.g.*, Ti4V6Al) have proved as favorable bioinert bone implant materials.¹² Although Ti itself does not possess osteopromotive properties, it is characterized by high corrosion resistance in physiological medium, excellent mechanical properties and biocompatibility with bone tissue (low allergenic effect and inflammation reaction).¹³

In order to avoid bone implant rejection, it is desirable to design bone implants in such a manner as to replicate the natural bone composition (HAP and collagen). Various natural polymers were investigated for this purpose, in order to enhance adhesion and antibacterial properties of HAP-based composites on titanium, including chitosan,¹¹ gelatin,¹⁴ collagen,¹⁵ alginate,^{16,17} hyaluronic acid¹⁸ and silk fibroin.¹⁹ Among them, chitosan (CS) has attracted the greatest attention due to unique cationic nature associated with its intrinsic antibacterial properties²⁰ and film-forming ability. In the form of composite coating with HAP

it improves adhesion properties to the substrate and at the same time reduces the HAP brittleness.²¹ The load-bearing capacity of HAP/polymer composites can be enhanced by introducing graphene (Gr) as nanofiller.¹¹ Graphene is a two-dimensional structure composed of single layer sp²-hybridized carbon atoms, possessing unique properties such as high specific area, excellent thermal and mechanical characteristics and favorable electrical conductivity, that can affect the features of the host material.²² Some recent findings have also pointed to the graphene role in biominerilization and implant integration process,^{23,24} as well as improved antibacterial activity of composites upon its addition.^{25,26}

Even though substantial research has been done in this field, the adhesion of bacteria to the implant surface and consequent bone infection still remains a critical issue to be solved. Biofilm formation and infection occurrence could be prevented by antibacterial agent addition that would act locally at the implantation site.²⁷ The antibacterial agent should be effective against a wide range of microorganisms and should express low cytotoxicity towards human cells. The antibacterial effect of silver and silver ions against a variety of microorganisms is well-documented.²⁸ The supposed antibacterial mechanism involves silver binding to cellular components, causing the cell membrane damage and interrupting the nucleic acid replication processes leading to cell death.^{28,29}

Clinical practice involves the systemic administration of antibiotics as a standard postoperative procedure after the implantation.³⁰ However, as a consequence, insufficient drug concentration is achieved at the injured site, leading to infection occurrence and bone implant rejection. An effective approach could represent local delivery of antibiotic at the targeted site, thus achieving high local drug concentration without causing a cytotoxic effect.^{31,32} Bone infection therapy usually includes gentamicin (Gent) due to its wide-spectrum action. It is a broad-spectrum antibiotic which is effective against most Gram-positive and Gram-negative bacteria.^{32,33} Orthopedic implant coatings, designed as antibiotic-release systems could overcome the problems associated with bone infections, with simultaneously controlled long-term antibiotic release at the targeted site.^{34,35}

Bearing in mind numerous demands that contemporary orthopedics is facing, it is essential to develop such non-cytotoxic composite coatings that would provide high load-bearing features with preferable antibacterial properties. Therefore, this paper represents a comprehensive review of electrophoretically deposited HAP-based composite coatings on titanium surface loaded with antibacterial agents.

2. ELECTROPHORETIC DEPOSITION OF HYDROXYAPATITE-BASED COMPOSITE COATINGS ON TITANIUM

Electrophoretic deposition was efficiently used for obtaining HAP-based composite coatings on titanium substrate intended for orthopedic implants

use.^{5,11,36} Besides simplicity and efficacy, this technique also enables obtaining uniform, homogenous and porous composites which are very important from the bioactivity view.^{37,38} Based on previously published data,^{5,11,21} EPD was performed from the three-electrode arrangement, consisting of two platinum panels as counter electrodes placed parallel to Ti foil that served as a working electrode. Thus, coating deposition on both sides of the Ti substrate was enabled, ensuring the homogeneity and uniformity of composite coatings.²¹

Pure HAP¹¹ and HAP-based composite coatings were deposited from ethanol suspensions – HAP/Gr,⁵ Ag/HAP,³⁹ Ag/HAP/Gr,³⁶ HAP/CS¹¹ and HAP/CS/¹¹ Gr and aqueous suspensions – HAP/CS²¹ and HAP/CS/Gent.²¹ Table I represents an overview of EPD operating conditions for HAP and HAP-based composite coatings on titanium substrate.

TABLE I. EPD parameters for HAP and HAP-based composite coatings

Suspension	Suspension composition	Deposition voltage, V	Deposition time, min	Solvent	Reference
HAP	1 wt. % HAP	60	0.5	Ethanol	11
HAP/Gr	1 wt. % HAP 0.01 wt. % Gr	60	2	Ethanol	5
Ag/HAP	1 wt. % nanosized Ag/HAP powder	60	0.75	Ethanol	40
Ag/HAP/Gr	1 wt. % nanosized Ag/HAP powder 0.01 wt. % Gr	60	2	Ethanol	36
HAP/CS	1 wt. % HAP 0.05 wt. % CS	60	3	Ethanol	11
HAP/CS/Gr	1 wt. % HAP 0.05 wt. % CS 0.01 wt. % Gr	60	3	Ethanol	11
HAP/CS	1 wt. % HAP 0.05 wt. % CS	5	12	Water	21
HAP/CS/Gent	1 wt. % HAP 0.05 wt. % CS 0.1 wt. % Gent	5	12	Water	21

2.1. FTIR analysis

The analysis of FTIR spectra (Fig. 1) for all investigated coatings electro-deposited on titanium (HAP, HAP/Gr, Ag/HAP, Ag/HAP/Gr, HAP/CS/Gr, HAP/CS and HAP/CS/Gent) revealed the characteristic bands for HAP, showing that the structure of hydroxyapatite remained preserved in composite coatings, as we have shown in our previously published papers.^{5,11,21,36,40}

Briefly, the FTIR spectra exhibited carbonate bands at ~1410 and ~1460 cm⁻¹ indicating the presence of substituted HAP because carbonate groups (CO₃²⁻) substitute phosphate and/or hydroxyl ions in HAP lattice, leading to the format-

ion of B- or AB-type substitution in HAP structure.^{5,11,21,36} As it was reported in the literature,^{41,42} carbonate-substituted apatite is known to be the main constituent of the bone mineral. After the introduction of chitosan and/or graphene in composite coatings, new bands that correspond to the skeletal vibration of Gr appeared at 1540 cm⁻¹ for Ag/HAP/Gr³⁶ and HAP/Gr⁵ coatings and at 1578 cm⁻¹ for HAP/CS/Gr coating,¹¹ while characteristic bands for CS appeared at 1640 cm⁻¹

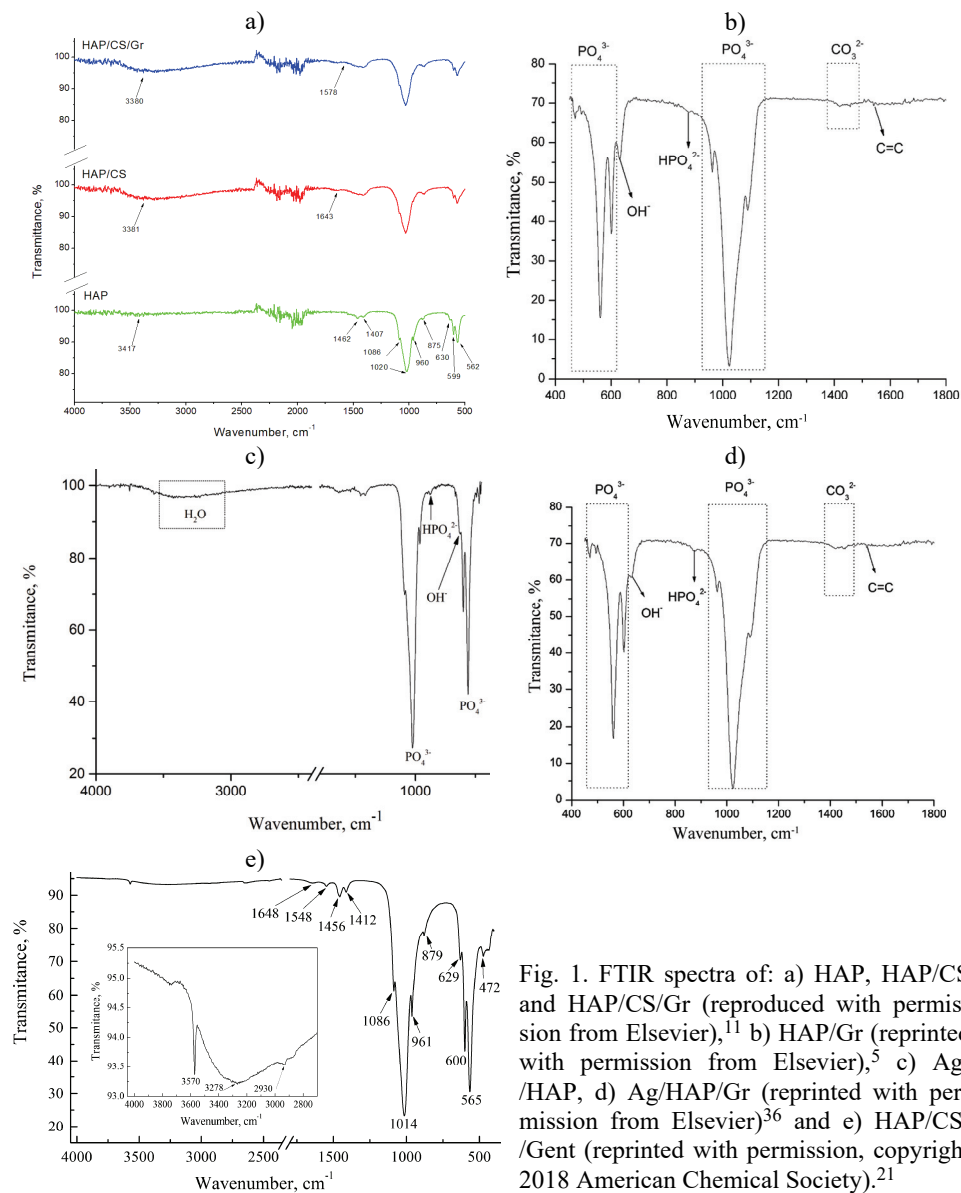


Fig. 1. FTIR spectra of: a) HAP, HAP/CS and HAP/CS/Gr (reproduced with permission from Elsevier),¹¹ b) HAP/Gr (reprinted with permission from Elsevier),⁵ c) Ag/HAP, d) Ag/HAP/Gr (reprinted with permission from Elsevier)³⁶ and e) HAP/CS/Gent (reprinted with permission, copyright 2018 American Chemical Society).²¹

(amide I band) for HAP/CS/Gr coating¹¹ and at 1546 (amide II band) and 1647 cm⁻¹ (amide I band) for HAP/CS and HAP/CS/Gent coatings,²¹ confirming their incorporation in the composite coatings. The interaction of chitosan with hydroxyapatite occurred *via* hydrogen bonding between –OH groups of HAP and –NH₂ and –OH groups of chitosan.²¹ According to the literature, the interaction of HAP with graphene sheets occurs due to the van der Waals bonding.⁴³

2.2. FE-SEM analysis

FE-SEM analysis was performed in order to investigate the morphology of deposited HAP and HAP-based composite coatings. Fig. 2 depicts the FE-SEM microphotographs of electrophoretically deposited HAP, HAP/Gr, Ag/HAP, Ag/HAP/Gr, HAP/CS, HAP/CS/Gr and HAP/CS/Gent coatings in order to assess the impact of chitosan, graphene, silver and gentamicin on the microstructure of electrodeposited composite coatings in comparison with pure HAP coating. As it can be observed, all electrodeposited coatings exhibited a porous, homogenous structure. Moreover, the presence of sphere-like crystallites of HAP organized into agglomerates of different sizes, from several tens to several hundred nanometers was noticeable.⁴⁴ Pure HAP coating contained a big, hollow pore at the surface, highlighting its porosity (Fig. 2a). After graphene addition in HAP/Gr coating (Fig. 2b) individual crystals (<50 nm) of rod-shaped HAP could be observed. Moreover, high specific area of graphene nanosheets contributed to the enhanced bonding strength between HAP and Gr, allowing increased contact area for bonding with the matrix.⁴⁵ When silver was added to HAP in Ag/HAP composite coating (Fig. 2c) more homogenous surface with small rod-like HAP crystals was observed.³⁶ Due to the well-known bonding mechanism of graphene with HAP lattice which inhibits crack propagation simultaneously with mechanical properties improvement, Gr was added to Ag/HAP coating. As expected, Gr addition reduced cracks in the case of Ag/HAP/Gr (Fig. 2d) compared to Ag/HAP.³⁶ At the same time, Ag/HAP/Gr coating exhibited a more dense surface, with evenly distributed HAP crystals.³⁶

After the chitosan addition to HAP (HAP/CS, Fig. 2e), a more homogeneous and fracture-free coating could be observed. Spherical HAP agglomerates were embedded in the chitosan polymer matrix, confirming strong interfacial interaction between HAP and chitosan, based on the hydrogen bonding between hydroxyl groups of CS and OH⁻, Ca²⁺ and PO₄³⁻ groups of HAP.⁴⁶ Comparing the morphology of pure HAP (Fig. 2a), HAP/CS (Fig. 2e) and HAP/CS/Gr (Fig. 2f), it could be noticed that the graphene caused significant improvement in HAP/CS/Gr coating morphology and porosity. HAP/CS/Gr coating exhibited a more compact surface attributed to Gr bonding to HAP and CS. Moreover, the high specific surface area of Gr increased the contact area with the HAP-polymer matrix, so it induced even distribution of HAP crystals in a polymer network and prevented the cracks appearance.^{18,36}

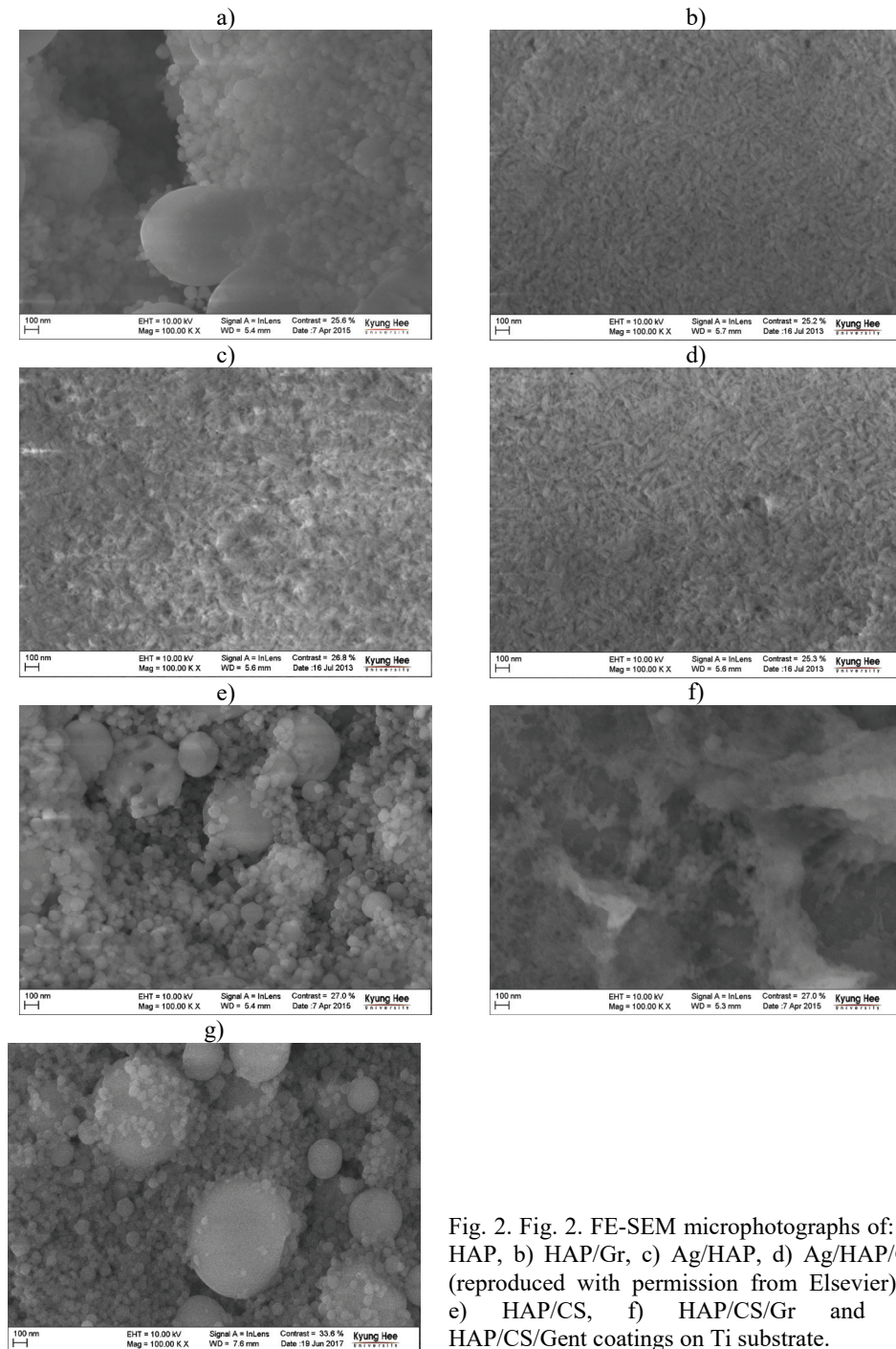


Fig. 2. Fig. 2. FE-SEM microphotographs of: a) HAP, b) HAP/Gr, c) Ag/HAP, d) Ag/HAP/Gr (reproduced with permission from Elsevier),³⁶ e) HAP/CS, f) HAP/CS/Gr and g) HAP/CS/Gent coatings on Ti substrate.

After the antibiotic incorporation in this coating (HAP/CS/Gent, Fig. 2g), no significant differences of surface morphology, compared to the HAP (Fig. 2a) and HAP/CS (Fig. 2e), could be observed, meaning that gentamicin addition did not alter the coating morphology. This is a consequence of gentamicin macromolecular structure, enabling the uniform distribution throughout the whole coating.²¹

2.3. XPS analysis

XPS analysis is a powerful method which can be used to assess the chemical surface composition of electrodeposited samples, as well as to calculate the Ca/P ratio, which is an important parameter for bioapplication of hydroxyapatite-based materials. Table II represents the quantitative chemical composition (at. %) for HAP, HAP/Gr, Ag/HAP, Ag/HAP/Gr, HAP/CS, HAP/CS/Gr and HAP/CS/Gent coatings on Ti.

TABLE II. Elemental surface composition (at. %) and Ca/P ratio of HAP, HAP/Gr, Ag/HAP, Ag/HAP/Gr, HAP/CS, HAP/CS/Gr and HAP/CS/Gent coatings based on XPS surface analysis

Signal	HAP	HAP/Gr	Ag/HAP	Ag/HAP/Gr	HAP/CS	HAP/CS/Gr	HAP/CS/Gent
C 1s	—	11.9	—	12.1	18.7	32.3	15.5
O 1s	57.6	51.3	58.0	51.0	51.4	43.6	54.8
P 2p	15.9	14.2	16.7	14.6	10.6	8.33	12.5
Ca 2p	26.3	22.5	17.0	15.0	17.4	14.5	15.1
N 1s	—	—	—	—	1.66	1.00	1.00
Ti 2p	0.21	0.09	0.14	0.14	0.19	0.09	—
Ag 3d	—	—	0.11	0.15	—	—	—
S 2p	—	—	—	—	—	—	1.00
Ca/P ratio	1.66	1.58	1.52	1.50	1.64	1.74	1.21
Reference	11	5	36	36	11	11	21

Comparing the results for elemental composition at the surface, a few differences have been observed allowing the comparisons among the given samples. As expected, pure HAP coating, as well as Ag/HAP coating, did not contain carbon and nitrogen in its surface composition. However, after chitosan, graphene and gentamicin addition these elements were observed, confirming their successful incorporation, while the highest value for C 1s content (32.3 at. %) was noticed for HAP/CS/Gr coating due to chitosan and graphene effect. Silver detection at the surface of Ag/HAP and Ag/HAP/Gr undoubtedly confirmed the Ag incorporation in the HAP crystal lattice. Similar Ag content (0.11 and 0.15 at. %) was calculated for both samples, Ag/HAP and Ag/HAP/Gr, respectively (Table II). The introduction of gentamicin into a HAP/CS/Gent coating caused the sulfur appearance at the surface at the same time indicating successful gentamicin loading.²¹ The absence of Ti 2p in the case of HAP/CS/Gent indicated the excellent coverage of the Ti substrate. Based on the XPS results, the Ca/P atomic ratios for HAP, HAP/CS and HAP/CS/Gr coatings were calculated to be 1.66, 1.64 and

1.74, respectively, indicating the stoichiometric HAP presence (theoretical Ca/P ratio = 1.67). However, the incorporation of silver in Ag/HAP and Ag/HAP/Gr coatings and gentamicin in HAP/CS/Gent coating, as well as Gr in HAP/Gr resulted in calculated Ca/P ratios of 1.52, 1.50, 1.21 and 1.58 respectively, indicating the calcium-deficient hydroxyapatite. As reported in the literature, Ca/P ratio for calcium-deficient hydroxyapatite is generally < 1.67 .^{47,48} Apparently, non-stoichiometry and lower Ca/P ratios (< 1.67) in HAP structure are due to the existence of adsorbed phosphate ions on the surface of the precipitated solids. These are the encouraging results since calcium-deficient hydroxyapatite is usually substituted with carbonate ions whereupon the „AB-type” carbonate hydroxyapatite would form. Having in mind that carbonate-substituted HAP possesses better osteopromotive and biomimetic properties compared to stoichiometric HAP, HAP/Gr, Ag/HAP, Ag/HAP/Gr and HAP/CS/Gent coating would be excellent candidates for future orthopedic implant use.^{21,36}

2.4. TG analysis

With the aim to investigate the thermal stability of pure HAP coating, as well as different HAP composite coatings (HAP/Gr, HAP/CS, Ag/HAP, Ag/HAP/Gr, HAP/CS/Gent and HAP/CS/Gr), electrodeposited on Ti substrate, the TG analyses were performed in the temperature interval from 25 to 600 °C (Fig. 3), while corresponding mass losses are represented in Table III.

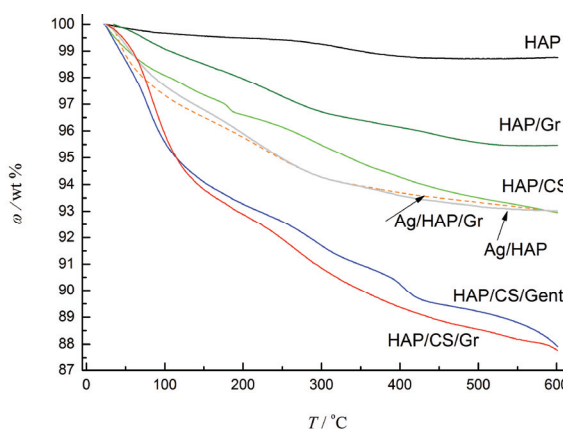


Fig. 3. TG curves, represented as temperature dependence of residual mass percent, ω , for HAP, HAP/CS, HAP/CS/Gent, Ag/HAP/Gr, HAP/Gr, Ag/HAP and HAP/CS/Gr coatings on Ti substrate.

Mass loss in the first temperature interval (25–200 °C) for all investigated coatings can be assigned to the desorption of physically adsorbed water^{5,11,21,36,40} and release of hydrogen-bonded water.⁴⁹ The highest value of mass loss in this temperature interval was obtained for HAP/CS/Gr and HAP/CS/Gent (7 wt. %),

while the lowest one was obtained for pure HAP coating (0.51 wt. %), indicating that Ag, CS, Gr and Gent introduction to the coatings caused the significant increase of adsorbed water, compared to the pure HAP coating.

TABLE III. Thermal behavior of HAP, HAP/Gr, HAP/CS, Ag/HAP, Ag/HAP/Gr, HAP/CS/Gent and HAP/CS/Gr coatings in the temperature interval from 25 to 600 °C

Coating	Mass loss, wt. %			Total mass loss (25–600 °C), wt. %
HAP	(25–200 °C) 0.51	(200–400 °C) 0.68	(400–600 °C) 0.05	1.24
HAP/Gr	(25–150 °C) 1.5	(150–350 °C) 2.1	(350–600 °C) 0.9	4.5
HAP/CS	(25–200 °C) 3.4	(200–500 °C) 2.5	(500–600 °C) 0.9	7
Ag/HAP	(25–150 °C) 3.2	—	(150–600 °C) 3.8	7
Ag/HAP/Gr	(25–150 °C) 3.39	(150–350 °C) 2.62	(350–600 °C) 1	7
HAP/CS/Gent	(25–200 °C) 7.0	(200–500 °C) 3.6	(500–600 °C) 0.9	12
HAP/CS/Gr	(25–200 °C) 7.0	(200–400 °C) 3.6	(400–600 °C) 1.6	12.2

Having in mind that the main component of all composite coatings is hydroxyapatite, the mass loss in the second temperature interval (200–400 °C) can be attributed to the beginning of HAP dehydroxylation process, along with decarbonation of HAP.^{5,11,21,36,40,50} When CS was introduced in the composite coatings (HAP/CS, HAP/CS/Gent and HAP/CS/Gr), decomposition of chitosan occurred below 300 °C.^{11,21,36,40,49} Additionally, melting of different gentamicin isoforms, *e.g.*, gentamicin thermal degradation occurred in the case of HAP/CS/Gent coating, falls into same temperature interval as well.^{21,51} Another phenomenon in this stage, specific for the Ag/HAP/Gr and HAP/Gr coatings is decomposing of unstable carbon in graphene structure.^{5,36,52} In the third temperature interval (400–600 °C) further heating of the coatings caused significant changes in the coatings structure. The mass loss in this temperature interval was assigned to the loss of carbonate ions from HAP structure, as CO₂ molecules,⁵⁰ along with degradation of residual cross-linked chitosan⁵³ and Gent degradation. It was reported that the thermal degradation of CS occurs mostly through the free radicals mechanism,⁴⁹ leading to the formation of a more stable cross-linked structure with respect to the linear chains. Such cross-linked structure decomposes at higher temperatures, being present in the char residue up to 600 °C.

According to the presented results, it could be concluded that all coatings exhibited good thermal stability in the investigated temperature interval. Although Gr addition caused a slight decrease in thermal stability, Gr-based coatings can be also considered thermally stable as graphene-free samples.

2.5. Antibacterial activity

The main objective of introducing a potent antibacterial agent as part of the coatings intended for usage as bone tissue implants had to be verified through their actual antibacterial activity. Therefore, electrodeposited HAP and HAP composite coatings were tested against the two most common culprits for bone infection occurrence – Gram-positive pathogenic bacteria *Staphylococcus aureus* and Gram-negative bacteria *Escherichia coli* by test in suspension.^{11,21}

Potential synergistic antibacterial effect of graphene and Ag as components of composite coatings of HAP/Gr and Ag/HAP/Gr was evaluated by monitoring antibacterial activity kinetics in suspension. Presence of the powerful antibacterial agents as silver and silver ions in the composites provided for desirable antibacterial effect, so Ag/HAP/Gr composite electrophoretically deposited on Ti had an immediate efficacy against *S. aureus* and *E. coli* (Fig. 4). After just 1 h of *S. aureus* exposure to Ag/HAP/Gr, reduction of cell numbers, *i.e.*, viability dropped for one logarithmic unit (72.9 % cell reduction), compared to the initial bacterial numbers. Complete reduction of bacteria cells of both *S. aureus* and *E. coli* was achieved after 24 h exposure to Ag/HAP/Gr, pointing to strong Ag antibacterial efficiency.³⁶ However, graphene initial concentration was too low to induce any antibacterial effect of HAP/Gr composite against both tested microorganisms (Fig. 4). The survival and propagation pattern of HAP/Gr coating followed closely the behavior of both bacterial strains in the control (bacteria only, no sample present).

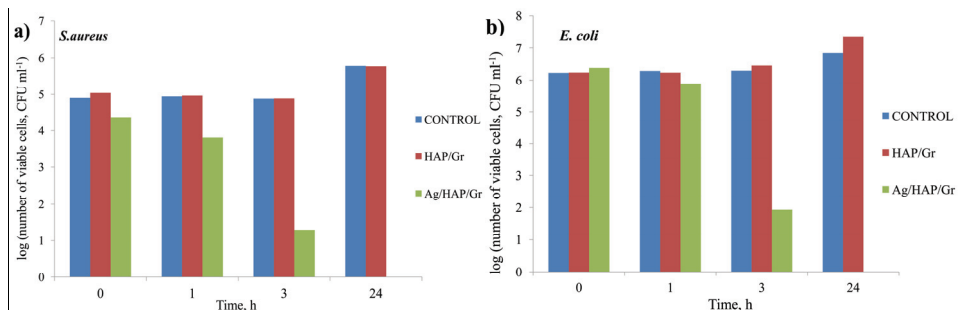


Fig. 4. Viable *S. aureus* (a) and *E. coli* (b) cell number reduction in the presence of HAP/Gr and Ag/HAP/Gr composite coatings.

Similar behavior was previously observed for Ag/HAP composite coating that expressed very strong bactericidal effect after 24 h incubation, causing complete reduction of cell colonies of tested *S. aureus* and *E. coli* bacteria.³⁹ In our studies, we have demonstrated that pure HAP coating unfortunately did not perturb bacterial growth of the tested strains.²¹ Therefore it is necessary that all

types of coated Ti surface would have to include the presence of a strong antibacterial agent.

Although silver acts immediately and efficiently, destroying *S. aureus* and *E. coli* after just 24 h, there is also a problem of potential toxicity towards healthy human cells due to the cumulative effect of silver if used for a prolonged period of time. In order to circumvent these side effects while retaining the desired antibacterial properties, another route was explored by replacing silver with another antibacterial agent – antibiotic gentamicin.

The impact of gentamicin addition and the subsequently improved antibacterial properties of HAP-based composites were monitored by antibacterial activity kinetics in suspension testing. The antibacterial assay for HAP, HAP/CS, HAP/CS/Gr and HAP/CS/Gent was conducted against *S. aureus* and *E. coli* and the obtained results are summarized in Table IV.

TABLE IV. Antibacterial activity of HAP and HAP-based coatings against Gram-positive *S. aureus* and Gram-negative *E. coli*

Bacteria	Time, h	log (number of viable cells, CFU/ml) ^{5,21}				
		Control	HAP	HAP/CS	HAP/CS/Gr	HAP/CS/Gent
<i>S. aureus</i>	0	5.36	5.65	4.83	5.92	2.84
	1	6.08	5.85	4.99	5.94	0.00
	3	6.31	6.12	5.22	6.34	0.00
	24	7.20	6.65	5.92	6.74	0.00
<i>E. coli</i>	0	5.97	6.06	6.30	6.20	6.12
	1	6.18	6.32	6.41	6.21	5.90
	3	6.67	6.65	6.52	6.68	5.28
	24	7.41	7.22	7.32	7.38	3.79

HAP, HAP/CS and HAP/CS/Gr did not exhibit any antibacterial potential against either bacteria after 24 h-exposure, demonstrating that chitosan and graphene concentrations were too low to express antibacterial effect.¹¹ However, HAP/CS/Gent coating expressed a strong bactericidal effect immediately after inoculation, reducing the initial cell number by two logarithmic units. The so-called “burst release” effect of antibiotic caused complete reduction of *S. aureus* within 1h-exposure. *E. coli* did not respond as well as *S. aureus*, but a noticeable reduction of cell numbers was observed after 24 h-exposure. Comparing the results of antibacterial testing, it was stated that HAP/CS/Gent induced bactericidal effect (more than 3 logarithmic units cell reduction) against *S. aureus* and bacteriostatic effect (less than 3 logarithmic units cell reduction) against *E. coli*.²¹ Having in mind broad-spectrum antibacterial effect of gentamicin, and good antibacterial testing results, Gent proved to be a good candidate for designing composite orthopedic implant coatings.

2.6. Cytotoxicity

Biocompatibility is one of the essential features that a certain biomaterial needs to fulfill, in order to comply with all the requirements in the biomedical field. The most common method for the cytotoxicity evaluation is *in vitro* 3-(4,5-dimethylthiazol-2-yl)-2,5-diphenyl tetrazolium bromide (MTT) testing towards different cell lines serving as “model system” in order to evaluate the impact of HAP-based composite coatings on healthy human cells. HAP, HAP/Gr, Ag/HAP, Ag/HAP/Gr, HAP/CS and HAP/CS/Gr coatings were subjected to MTT cytotoxicity testing towards peripheral blood mononuclear cells (PBMC), composed of lymphocytes and monocytes (human immune system components) before proceeding to osteosarcoma cells (tissue-specific for orthopedic implants).^{5,11,36} Fig. 5 represents the cytotoxicity results for HAP, HAP/CS and HAP/CS/Gr composites towards PBMC cell line with and without the addition of proliferation-stimulating factors (PHA).

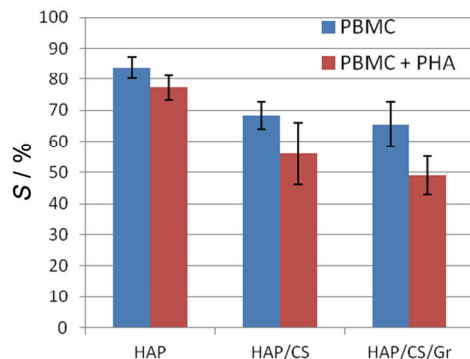


Fig. 5. Reduction of PBMC cell viability in the presence of HAP, HAP/CS and HAP/CS/Gr coatings. Reprinted with permission from Elsevier.¹¹

HAP, HAP/CS and HAP/CS/Gr coatings caused a mild decrease in the PBMC cell survival compared to the control sample. According to the cytotoxicity scale adapted from Sjogren *et al.*,⁵⁴ it could be safe to state that these coatings did not cause a cytotoxic effect on the surrounding tissue. After proliferation stimulation, a slight decrease of cell viability was observed for all samples.

When cytotoxicity was tested towards PMBC in the presence of Ag/HAP, HAP/Gr and Ag/HAP/Gr, a decrease of healthy immunocompetent PBMC cell survival up to $94.6 \pm 4.2\%$ for Ag/HAP,³⁹ $72.3 \pm 4.3\%$ for HAP/Gr⁵ and $79.6 \pm 11.2\%$ for Ag/HAP/Gr³⁶ compared to the control ($S = 100\%$) was calculated. According to the classification found in literature,⁵⁵ all investigated samples could be declared as non-cytotoxic against target PBMC. Having in mind that PBMC cells are the first line of immune defense against any type of implant in the human body, obtained results were encouraging for further investigations.

Cytotoxicity of HAP/CS and HAP/CS/Gent coatings (Fig. 6) were tested against MRC-5 (human fibroblast cell line) and L929 (mice fibroblast cell line), serving as a model system before proceeding to tissue-specific osteosarcoma cells.

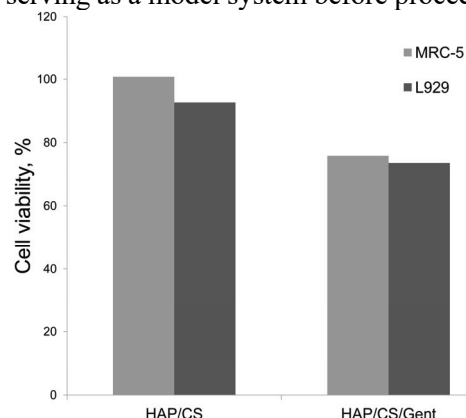


Fig. 6. Cell viability of MRC-5 and L929 cells in the presence of HAP/CS and HAP/CS/Gent. Reprinted with permission. Copyright 2018 American Chemical Society.²¹

As expected, human MRC-5 cell line responded better in this assay for both composite samples causing a smaller reduction of cell survival compared to the L929 cell line which exhibited increased sensitivity. Comparing the results for HAP/CS and HAP/CS/Gent coating it was observed that HAP/CS/Gent expressed higher reduction rate of cell survival compared to HAP/CS for both tested cell lines. According to these results, HAP/CS composite coating could be classified as non-cytotoxic, while HAP/CS/Gent could be characterized as mildly cytotoxic, but still a good candidate for medical use.²¹

3. CONCLUSION

This paper presents a comprehensive review of electrophoretically deposited pure HAP and HAP-based composite coatings with chitosan and graphene with antibacterial agents, silver and gentamicin, *i.e.* Ag/HAP, HAP/Gr, Ag/HAP/Gr, HAP/CS, HAP/CS/Gr and HAP/CS/Gent. Successful deposition of all investigated composite coatings was demonstrated by FTIR analysis. Characteristic bands for HAP confirmed that HAP retained its structure in all investigated composite coatings, while the carbonate bands proved the substituted HAP. FE-SEM exhibited uniform homogenous surface of high porosity, capable of providing enhanced biointegration process of bone implant with the surrounding tissue. Graphene had a favourable effect on the morphology of electrodeposited samples, inhibiting the crack propagation and serving as reinforcement filler. TGA analysis confirmed good thermal properties for all investigated samples, emphasizing the stable structure of all deposited HAP-based composite coatings. Antibacterial properties of HAP-based coatings were estimated by test in suspension against *S. aureus* and *E. coli*. Composite coatings without antibacterial agents (HAP, HAP/Gr, HAP/CS and HAP/CS/Gr) did not express any antibac-

terial effect against tested microorganisms. The loaded amount of CS and Gr was not sufficient to exhibit antibacterial activity and no reduction of tested bacteria was observed after 24 h-exposure. However, silver addition significantly improved the antibacterial activity of composites. Within only 3 h exposure, Ag/HAP and Ag/HAP/Gr completely diminished bacterial cells in the suspension, proving Ag antibacterial efficacy against both tested bacteria. The addition of antibiotic gentamicin caused even better antibacterial efficacy in the case of *S. aureus*. Complete bacteria reduction was achieved within only 1 h exposure, demonstrating the powerful Gent antibacterial effect against Gram-positive *S. aureus*. On the other hand, Gent antibacterial effect was less pronounced against *E. coli*, and the antibacterial effect could be classified as “bacteriostatic” (less than two logarithmic units reduction). Biocompatibility of HAP-based coatings was confirmed using MTT testing proving non-cytotoxic effect towards healthy human PBMC, MRC-5 and mice L929 cell lines.

Acknowledgments. This work was supported by the Ministry of Education, Science and Technological Development of Serbia, Grant No. III45019 and Basic Science Research Program through the National Research Foundation of Korea (NRF) funded by the Ministry of Education, Science and Technology (project No 2018R1A2B5A02023190).

ИЗВОД

ЕЛЕКТРОФОРЕТСКЕ КОМПОЗИТНЕ ПРЕВЛАКЕ НА БАЗИ ХИДРОКСИАПАТИТА СА СРЕБРОМ И ГЕНТАМИЦИНОМ КАО АНТИБАКТЕРИЈСКИМ АГЕНСИМА

МИЛЕНА СТЕВАНОВИЋ¹, МАРИЈА ЂОШИЋ², АНА ЈАНКОВИЋ¹, KYONG YOP RHEE³
и ВЕСНА МИШКОВИЋ-СТАНКОВИЋ¹

¹Технолошко-мешалуршки факултет, Универзитет у Београду, Карнеџијева 4, Београд, ²Институт за технологију нуклеарних и других минералних сировина (ИТНМС), Булевар Франши г'Енереа 86, Београд и ³Department of Mechanical Engineering, Kyung Hee University, Yongin 449-701, South Korea

Све већа потреба за побољшаним, биокомпатабилним имплантатима коштаног ткива довела је до интензивних истраживања нових биоматеријала, посебно нових композитних превлака на бази хидроксипатита (HAP) на површини титана и легура титана. Због одличне биокомпабилности и остеоиндуктивних својстава, хидроксипатит се често користи као део композитних биоматеријала намењених за примену у ортопедским имплантатима. У циљу превазилажења проблема бактеријске инфекције испитивани су различити антимикробни агенси и материјали, као и њихова инкорпорација у таква медицинска средства. Овај рад представља свеобухватан преглед електрофоретског таложења у једном ступњу композитних превлака хидроксипатит/хитозан/графен са сребром и антибиотиком гентамицином, као антибактеријским агенсима, на титану. Побољшање механичких и адхезивних својстава композитних превлака постигнуто је додатком графена и хитозана, док су пожељне антибактеријске особине добијене додатком гентамицина и сребра. Биокомпабилност електрофоретских НАР и композитних превлака на бази НАР процењена је МТТ тестом указујући на нецитотоксични ефекат и висок потенцијал за будућу медицинску употребу у виду превлака за ортопедске имплантате.

(Примљено 21. августа, прихваћено 28. августа 2019)

REFERENCES

1. O. O. Van der Biest, L. J. Vandeperre, *Ann. Rev. Mater. Sci.* **29** (1999) 327 (<http://dx.doi.org/10.1146/annurev.matsci.29.1.327>)
2. L. Besra, M. Liu, *Prog. Mater. Sci.* **52** (2007) 1 (<http://dx.doi.org/10.1016/j.pmatsci.2006.07.001>)
3. I. Zhitomirsky, L. Gal-Or, *J. Mater. Sci. Mater. Med.* **8** (1997) 213 (<http://dx.doi.org/10.1023/A:1018587623231>)
4. H. Qi, S. Heise, J. Zhou, K. Schuhladen, Y. Yang, N. Cui, R. Dong, S. Virtanen, Q. Chen, A. R. Boccaccini, T. Lu, *ACS Appl. Mater. Interfaces* **11** (2019) 8625 (<http://dx.doi.org/10.1021/acsami.9b01227>)
5. A. Janković, S. Eraković, M. Mitić, I. Z. Matić, Z. D. Juranić, G. C. P. Tsui, C. Tang, V. Mišković-Stanković, K. Y. Rhee, S. J. Park, *J. Alloys Compd.* **624** (2015) 148 (<http://dx.doi.org/10.1016/j.jallcom.2014.11.078>)
6. S. Heise, C. Forster, S. Heer, H. Qi, J. Zhou, S. Virtanen, T. Lu, A. R. Boccaccini, *Electrochim. Acta* **307** (2019) 318 (<http://dx.doi.org/10.1016/j.electacta.2019.03.145>)
7. E. Avcu, F. E. Baştan, H. Z. Abdullah, M. A. U. Rehman, Y. Y. Avcu, A. R. Boccaccini, *Prog. Mater. Sci.* **103** (2019) 69 (<http://dx.doi.org/10.1016/j.pmatsci.2019.01.001>)
8. W. R. Lacefield, *Ann. N. Y. Acad. Sci.* **523** (1988) 72 (<http://dx.doi.org/10.1111/j.1749-6632.1988.tb38501.x>)
9. W. Suchanek, M. Yoshimura, *J. Mater. Res.* **13** (2017) 94 (<http://dx.doi.org/10.1557/JMR.1998.0015>)
10. H. Zhou, J. Lee, *Acta Biomater.* **7** (2011) 2769 (<http://dx.doi.org/10.1016/j.actbio.2011.03.019>)
11. M. Đošić, S. Eraković, A. Janković, M. Vukašinović-Sekulić, I. Z. Matić, J. Stojanović, K. Y. Rhee, V. Mišković-Stanković, S. J. Park, *J. Ind. Eng. Chem.* **47** (2017) 336 (<http://dx.doi.org/10.1016/j.jiec.2016.12.004>)
12. L. Zhao, P. K. Chu, Y. Zhang, Z. Wu, *J. Biomed. Mater. Res., B: Appl. Biomater.* **91** (2009) 470–480 (<http://dx.doi.org/10.1002/jbm.b.31463>)
13. B. Kasemo, *Interface* **49** (1983) 832 ([http://dx.doi.org/10.1016/0022-3913\(83\)90359-1](http://dx.doi.org/10.1016/0022-3913(83)90359-1))
14. F. Frajkorová, E. Molero, P. Montero, M. C. Gomez-Guillen, A. J. Sanchez-Herencia, B. Ferrari, *J. Eur. Ceram. Soc.* **36** (2016) 343 (<http://dx.doi.org/10.1016/j.jeurceramsoc.2015.07.005>)
15. A. Tozar, İ. H. Karahan, *Surf. Coatings Technol.* **340** (2018) 167 (<http://dx.doi.org/10.1016/j.surfcoat.2018.02.034>)
16. V. Ozhukil Kollath, Q. Chen, S. Mullens, J. Luyten, K. Traina, A. R. Boccaccini, R. Cloots, *J. Mater. Sci.* **51** (2016) 2338 (<http://dx.doi.org/10.1007/s10853-015-9543-6>)
17. Q. Chen, L. Cordero-Arias, J. A. Roether, S. Cabanas-Polo, S. Virtanen, A. R. Boccaccini, *Surf. Coatings Technol.* **233** (2013) 49 (<http://dx.doi.org/10.1016/j.surfcoat.2013.01.042>)
18. M. Li, Q. Liu, Z. Jia, X. Xu, Y. Shi, Y. Cheng, Y. Zheng, T. Xi, S. Wei, *Appl. Surf. Sci.* **284** (2013) 804 (<http://dx.doi.org/10.1016/j.apsusc.2013.08.012>)
19. Z. Zhong, J. Ma, *J. Biomater. Appl.* **32** (2017) 399 (<http://dx.doi.org/10.1177/0885328217723501>)
20. D. Raafat, H. G. Sahl, *Microb. Biotechnol.* **2** (2009) 186 (<http://dx.doi.org/10.1111/j.1751-7915.2008.00080.x>)
21. M. Stevanović, M. Đošić, A. Janković, V. Kojić, M. Vukašinović-Sekulić, J. Stojanović, J. Odović, M. Crevar Sakač, K. Y. Rhee, V. Misković-Stanković, *ACS Biomater. Sci. Eng.* **4** (2018) 3994 (<http://dx.doi.org/10.1021/acsbiomaterials.8b00859>)

22. S. Stankovich, D. A. Dikin, G. H. B. Dommett, K. M. Kohlhaas, E. J. Zimney, E. A. Stach, R. D. Piner, S. B. T. Nguyen, R. S. Ruoff, *Nature* **442** (2006) 282 (<http://dx.doi.org/10.1038/nature04969>)
23. M. Zhang, Y. Li, Z. Su, G. Wei, *Polym. Chem.* **6** (2015) 6107 (<http://dx.doi.org/10.1039/c5py00777a>)
24. Y. Chen, Y. Feng, J. G. Deveaux, M. A. Masoud, F. S. Chandra, H. Chen, D. Zhang, L. Feng, *Minerals* **9** (2019) 68 (<http://dx.doi.org/10.3390/min9020068>)
25. S. Liu, T. H. Zeng, M. Hofmann, E. Burcombe, J. Wei, R. Jiang, J. Kong, Y. Chen, *ACS Nano* **5** (2011) 6971 (<http://dx.doi.org/10.1021/mn202451x>)
26. H. M. Hegab, A. Elmekawy, L. Zou, D. Mulcahy, C. P. Saint, M. Ginic-Markovic, *Carbon* **105** (2016) 362 (<http://dx.doi.org/10.1016/j.carbon.2016.04.046>)
27. J. Hasan, R. J. Crawford, E. P. Ivanova, *Trends Biotechnol.* **31** (2013) 295 (<http://dx.doi.org/10.1016/j.tibtech.2013.01.017>)
28. M. Guzman, J. Dille, S. Godet, *Nanomedicine Nanotechnology, Biol. Med.* **8** (2012) 37 (<http://dx.doi.org/10.1016/j.nano.2011.05.007>)
29. K. J. Woo, C. K. Hye, W. K. Ki, S. Shin, H. K. So, H. P. Yong, *Appl. Environ. Microbiol.* **74** (2008) 2171 (<http://dx.doi.org/10.1128/AEM.02001-07>)
30. L. Prokuski, *J. Am. Acad. Orthop. Surg.* **16** (2008) 283 (<http://dx.doi.org/10.5435/00124635-200805000-00007>)
31. V. Antoci, C. S. Adams, N. J. Hickok, I. M. Shapiro, J. Parvizi, *Clin. Orthop. Relat. Res.* (2007) 200 (<http://dx.doi.org/10.1097/BLO.0b013e31811ff866>)
32. A. D. Hanssen, *Clin. Orthop. Relat. Res.* (2005) 91 (<http://dx.doi.org/10.1097/01.blo.0000175713.30506.77>)
33. A. Rudin, A. Healey, C. A. Phillips, D. W. Gump, B. R. Forsyth, *Med. Clin. North Am.* **54** (1970) 1305 ([http://dx.doi.org/10.1016/S0025-7125\(16\)32596-2](http://dx.doi.org/10.1016/S0025-7125(16)32596-2))
34. K. Kanellakopoulou, E. J. Giamarellos-Bourboulis, *Drugs* **59** (2000) 1223 (<http://dx.doi.org/10.2165/00003495-200059060-00003>)
35. J. R. Porter, T. T. Ruckh, K. C. Popat, *Biotechnol. Prog.* **25** (2009) 1539 (<http://dx.doi.org/10.1002/btpr.246>)
36. A. Janković, S. Eraković, M. Vukašinović-Sekulić, V. Mišković-Stanković, S. J. Park, K. Y. Rhee, *Prog. Org. Coat* **83** (2015) 1 (<http://dx.doi.org/10.1016/j.porgcoat.2015.01.019>)
37. L. Xu, F. Pan, G. Yu, L. Yang, E. Zhang, K. Yang, *Biomaterials* **30** (2009) 1512 (<http://dx.doi.org/10.1016/j.biomaterials.2008.12.001>)
38. B. G. X. Zhang, D. E. Myers, G. G. Wallace, M. Brandt, P. F. M. Choong, *Int. J. Mol. Sci.* **15** (2014) 11878 (<http://dx.doi.org/10.3390/ijms150711878>)
39. S. Eraković, A. Janković, I. Z. Matić, Z. D. Juranić, M. Vukašinović-Sekulić, T. Stevanović, V. Miskovic-Stankovic, *Mater. Chem. Phys.* **142** (2013) 521 (<http://dx.doi.org/10.1016/j.matchemphys.2013.07.047>)
40. A. Janković, S. Eraković, A. Dindune, D. Veljović, T. Stevanović, D. Janačković, V. Miskovic-Stankovic, *J. Serb. Chem. Soc.* **77** (2012) 1609 (<http://dx.doi.org/10.2298/JSC120712086J>)
41. S. M. Barinov, J. V. Rau, S. N. Cesaro, J. Čurišin, I. V. Fadeeva, D. Ferro, L. Medvecky, G. Trionfetti, *J. Mater. Sci. Mater. Med.* **17** (2006) 597 (<http://dx.doi.org/10.1007/s10856-006-9221-y>)
42. C. C. Wu, S. Te Huang, T. W. Tseng, Q. L. Rao, H. C. Lin, *J. Mol. Struct.* **979** (2010) 72 (<http://dx.doi.org/10.1016/j.molstruc.2010.06.003>)
43. Y. Liu, J. Huang, H. Li, *J. Mater. Chem. B* **1** (2013) 1826 (<http://dx.doi.org/10.1039/c3tb00531c>)

44. M. Djošić, V. Panić, J. Stojanović, M. Mitrić, V. Mišković-Stanković, *Colloids Surfaces A Physicochem. Eng. Asp.* **400** (2012) 36 (<http://dx.doi.org/10.1016/j.colsurfa.2012.02.040>)
45. V. Mišković-Stanković, A. Janković, S. Eraković, K. Yop Rhee, *Eurasian Chem. J.* **17** (2014) 3 (<http://dx.doi.org/10.18321/ectj189>)
46. E. M. El-Sayed, A. Omar, M. Ibrahim, W. I. Abdel-Fattah, *J. Comput. Theor. Nanosci.* **6** (2009) 1663 (<http://dx.doi.org/10.1166/jctn.2009.1228>)
47. K. Ishikawa, P. Ducheyne, S. Radin, *J. Mater. Sci. Mater. Med.* **4** (1993) 165 (<http://dx.doi.org/10.1007/BF00120386>)
48. E.E. Berry, *J. Inorg. Nucl. Chem.* **29** (1967) 317 ([https://doi.org/10.1016/0022-1902\(67\)80033-2](https://doi.org/10.1016/0022-1902(67)80033-2))
49. J. Zawadzki, H. Kaczmarek, *Carbohydr. Polym.* **80** (2010) 395 (<http://dx.doi.org/10.1016/j.carbpol.2009.11.037>)
50. T. I. Ivanova, O. V. Frank-Kamenetskaya, A. B. Kol'tsov, V. L. Ugolkov, *J. Solid State Chem.* **160** (2001) 340 (<http://dx.doi.org/10.1006/jssc.2000.9238>)
51. R. P. Aquino, R. Adami, S. Liparoti, G. Della Porta, *Int. J. Pharm.* **440** (2013) 188 (<http://dx.doi.org/10.1016/j.ijpharm.2012.07.074>)
52. V. Loryuenyong, K. Totepvimarn, P. Eimburanaprat, W. Boonchompoo, A. Buasri, *Adv. Mater. Sci. Eng.* (2013) 1 (<http://dx.doi.org/10.1155/2013/923403>)
53. F. A. López, A. L. R. Merce, F. J. Alguacil, A. López-Delgado, *J. Therm. Anal. Calorim.* **91** (2008) 633 (<http://dx.doi.org/10.1007/s10973-007-8321-3>)
54. G. Sjögren, G. Sletten, E. J. Dahl, *J. Prosthet. Dent.* **84** (2000) 229 (<http://dx.doi.org/10.1067/mpr.2000.107227>)
55. C. McManamon, J. P. De Silva, P. Delaney, M. A. Morris, G. L. W. Cross, *Mater. Sci. Eng., C* **59** (2016) 102 (<http://dx.doi.org/10.1016/j.msec.2015.09.103>).